Automatic Leg Regeneration for Robot Mobility Recovery

Liyu Wang and Ronald S. Fearing

***Abstract*— Automatic repair of mechanical structures would enable a robot to recover or improve functions after physical damage. Little work exists on real-world execution of automatic repair in robotic systems. State-of-the-art takes a modular approach where the robotic system is modular and a replacement module is available. However, the modular approach suffers from low granularity in repair even with tens of motors. In addition, there is a lack of quantitative evaluation of the effect of automatic repair on robot functionality. Here we propose a cooperative method for automatic repair in a robotic system. Our method is regeneration-based rather than module-based and does not assume availability of a replacement part. It integrates a fabrication process on the fly for robot structure regeneration. With a system that consists of a regenerating robot, a legged robot and a pre-engineered ribbon, we demonstrate end-to-end execution of automated repair of the legged robot's leg by the regenerating robot in 335 seconds. Experiments on repeatability show a 100% success rate for sub-processes such as positioning, leg fabrication, and legged robot disengagement and a 90% success rate for leg detachment. We quantify the effect of leg regeneration on mobility recovery and found a 90% recovery of forward speed, a 19.7% increase of peak power and a 9.3% reduction of cost of transport with a regenerated leg.**

I. Introduction

Automatic repair would enable a robotic system to recover functions after structural damage. There has been little work in real-world execution of automatic repair for robotic systems due to the complexity of the repairing itself. State-of-the-art uses a modular approach, where a faulty module is replaced by the rest of the modular system or by another modular robot with the supply of a replacement module. In contrast natural organisms utilize regeneration for recovery from a wound or loss of body parts. Although natural regeneration bears similarity to the modular approach at the cellular level, it is more appropriate to be viewed as a structure generation process at the macroscopic scale.

Regeneration is a capability which robotic systems are yet to have. The concept of a regenerative robotic system extends developmental robotics from cognitive level [1] to the physical level. It overlaps with other biologically-inspired concepts such as morphogenetic robotics [2] and robotic extended-phenotypes [3], but differs in (1) implementation techniques, which involves on-the-fly structure construction, and/or (2) purposes, which is function recovery or improvement.

A. Automatic repair in robotics

Automatic repair in a robotic system may be broken down to at least three steps: diagnosis, planning and execution [11].

*This work was supported by the Swiss National Science Foundation Postdoc Mobility Fellowship

Liyu Wang and Ronald S. Fearing are with Department of Electrical Engineering and Computer Sciences, University of California, Berkeley, CA 94720, USA liyu.wang@wadh.oxon.org

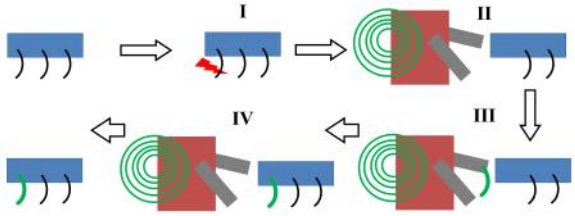

Fig. 1. Conceptual illustration of cooperative repair in a robotic system. I: Structure damage. II: Damaged robot and repairing robot approaching each other. III: Repairing robot regenerating a structure. IV: Repairing robot fixing the damaged robot with the regenerated structure.

TABLE I
Comparison of Related Methods

Ref.	No. motors	Minimal repair (mm)	Detach	On-the-fly fabrication	Attach	Robot function
[21]	33	125	Auto	None	Auto	2D display
[11]	12	240	Manual	None	Auto	Bipedal
[23]	8	132	Auto	None	Auto	2D display
Ours	10	30	Auto	Auto	Auto	Hexapedal

To our knowledge, no existing robotic system is capable of having all the three steps automated. A rich body of research exists for automatic fault diagnosis in robotics [12]. For automatic planning, algorithms have been developed for replacement of a module in modular self-reconfigurable (MSR) robots [14], [15], [16], [17] or restoration of formation control in a swarm of mobile robots [18], [19], [20].

Real-world execution of automatic replacement of mechanical systems are rare. To the best of our knowledge, three authors have addressed execution of automatic repair in a robotic system. Yoshida et al. [21] showed a MSR robotic system with a triangle structure formed by ten "Fractum" modules and an additional replacement module (11 in total). When one of the modules became defective, the fault would be automatically diagnosed by its neighbour(s). The replacement module, which was initially connected to the triangle, would move over to fill the space. Yim et al. showed another MSR robotic system with three clusters of four"CKbot" modules and a camera module (15 in total) [11]. The system became disconnected due to a manually applied external force but the three clusters remained intact and functional. Once the whole system was self-reassembled, it self-righted and resumed bipedal walking. Davis et al. demonstrated a case study towards team repair in a system of two robots [23]. Each robot consists of a central hub and seven heterogeneous modules. When a module became

hypothetically "faulty", the other robot would locate and orient to the "faulty" module, connect to it, and disconnect it from the rest of the first robot. No effort was needed to disconnect the "faulty" module or to search and connect the replacement module.

Table I compares these related methods to the present work. Here minimal repair refers to the size of the replaced or repaired structure. In general, previous work on automatic repair (1) assumes existence of replacement modules or parts and no fabrication of parts is present; (2) has a mixed level of automation for execution; and (3) lacks systematic study to show quantitative effects of repair afterwards.

B. Automatic Construction of Robot Structures

A key character of regeneration in robotics is structure construction on-the-fly. In theory this may be done by integrating fabrication processes and subsystems into a robot. In practice automatic construction of robot structures is distinct from rapid prototyping such as 3D printing where manual assembly is needed. Automatic construction of robot structure requires automatic assembly or no manual assembly. Nevertheless, 3D printing has the potential to become a method for robot regeneration, because it can fabricate various structures with a sufficiently fine granularity of 10-100 μm, although solutions to automatic detachment of a fabricated structure from the building plate as well as surface finish are yet to be proposed.

MacCurdy et al. used a commercial 3D printer and mutiple materials for automatic construction of robot structures [24]. Several structures were demonstrated with the most complex being the structure for a hexapedal robot. The structure was fabricated in one piece. Once manually assembled with a DC motor, a sensor, a microcontroller and a battery, the 14-cm long robot was able to walk 0.125 body-lengths per second. Brodbeck and Wang et al. used robot arms equipped with a hot-melt adhesive (HMA) dispensing unit for automatic construction of end-effectors [25], [26]. The robot arms functioned as a 3D printer for automatic fabrication as well as a manipulator for automatic assembly of HMA structures. These robot structures were later automatically attached to the robot arms and became end-effectors. A few structures were demonstrated for pick-and-place tasks, including a two-part scoop and a one-piece passive gripper.

C. Contribution and Outlines

This paper presents a method for automatic leg regeneration for robot mobility recovery. The contribution of the work is two fold. First, execution with the proposed method is demonstrated and repeatability is evaluated. Two, the effect of automatic leg regeneration on mobility recovery is quantified in terms of speed, power and locomotion efficiency.

The rest of the paper is organized as follows. Section II describes the regenerative robotic system. Section III presents a mathematical model for stiffness of flexure joints formed by the ribbon. Section IV presents experiments and results. Section V draws conclusions and points out future work.

II. A Regenerative Robotic System

We propose a robotic system that is capable of automatic leg regeneration. The system consists of a pre-engineered ribbon, a regenerating robot, and a hexapedal mobile robot, as shown in Fig. 2. Cooperatively the regenerating robot can regenerate the leg for the legged robot through on-the-fly fabrication based on ribbon folding. The ribbon folding fabrication method has been formulated in a scheme of folding in our previous work [27]. Demonstrated structures include 2D shapes, planar four-bar linkages, and simple 3D structures. In addition, motion planning has been suggested for single-ended sequential ribbon folding [28].

A. Ribbon

The ribbon is pre-engineered as a sandwich structure. For most parts it has five layers. In the middle there is a layer of polyethylene terephthalate (PET). Outside the PET layer there is a layer of paperboard on each side. These three layers are the same as in our previous work [27]. A layer of hot-melt adhesive (HMA) is added outside the paperboard layer on each side. The five-layer parts of the ribbon would function as relatively rigid links in a folded structure.

Three types of functional components exist for certain parts of the ribbon by having designated layers absent. As shown in Fig. 3, when paperboard layers are absent, the part becomes a shape-keeping joint; when HMA layers and paperboard layers are absent, it becomes a free-moving flexure hinge; and when only PET layer is absent, it becomes a terminating end. For the shape-keeping joint, HMA can be automatically heated, folded and cooled, and the joint will change its resting angle. For the terminating end, once HMA is heated the ribbon will break into two pieces and this is used for automatic detachment of a folded structure.

The ribbon is prepared by a modified version of the smart composite microstructures (SCM) fabrication process [29] i.e. with the addition of a manual HMA application process. In this study the thickness of each layer of the ribbon was as follows: PET layer, 0.05 mm; paperboard layer, 0.35 mm; HMA layer, 0.9 mm. All the three functional components had a gap of 1 mm long.

B. A Regenerating Robot

The regenerating robot consists of two units and is controlled with an Arduino Leonardo board.

1) Positioning and Orienting Unit: This unit automates four tasks: engaging, positioning, orienting the robot to be repaired, as well as detaching any remnant from the damaged leg from the robot. It realizes all these with four degrees-of-freedom (DOF) actuated by five motors (Fig. 2 right). The 3D positioning is achieved by two translational DOF in the horizontal plane and a rotational DOF in the vertical plane, actuated by three stepper motors (M4-M6) and a servo motor (M7) respectively. Orientation is achieved by a rotational DOF in the horizontal plane with a servo motor (M8).

A proximity sensor is used to detect if the damaged robot is physically engaged, and functions as a trigger for the regenerating robot to enter the regeneration sequence. A

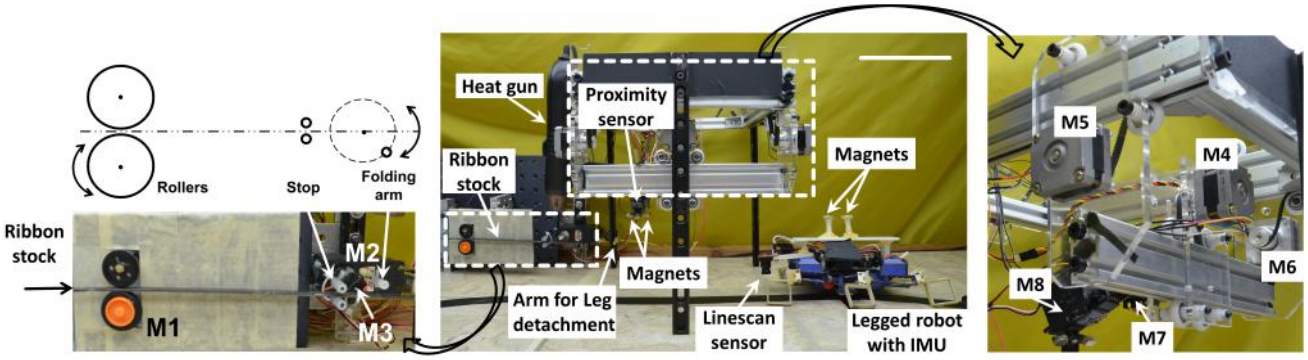

Fig. 2. A robotic system that is capable of automated leg regeneration. The system has a regenerating robot and a legged mobile robot. The regenerating robot has a fabrication unit (left) and a positioning and orienting unit (right). The fabrication unit uses three motors (M1-M3) to deliver and fold a pre-engineered ribbon into planar or 3D structures. The positioning and orienting unit uses five motors (M4-M8) to position and orient the legged robot. Communication between the two robots are enabled by a proximity sensor on the regenerating robot and an IMU onboard the legged robot. Physical engagement between the robots are enabled by two pairs of magnets. The white bar represents 10 cm in the middle figure.

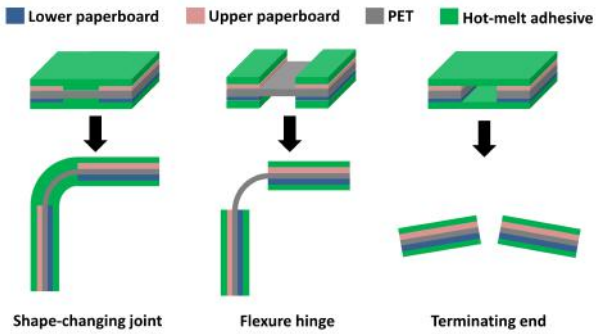

Fig. 3. Three types of functional components on the ribbon.

pair of permanent magnets are located on the horn of the servo motor responsible for orientation (M8). These magnets provide the force needed for engagement with the other robot, and act as a passive alignment mechanism between the two robots.

A rigid metal arm is mounted in a designated location on the regenerating robot and serves as a stop to provide a separation force to detach the remnant of a damaged leg, when the four positioning motors (M4-M7) drag the legged robot away from it.

2) Fabrication Unit: The unit was designed to fold the pre-engineered ribbon into planar linkages and structures. As shown in Fig. 2 left, it consists of four components i.e. a pair of rollers for feeding the ribbon, an arm for folding the ribbon, a heat gun to heat the HMA layers of the ribbon, and a stop that ensures the ribbon is only folded at the target location (in most cases at shape-changing joints).

The unit improves over our previous prototype [27] with better automation and precision. One of the rollers is actuated by a stepper motor (M1) while the other is passive. The folding arm is a 3.5cm-long metallic screw and is actuated by two servos: a sail winch servo (M2) for position-controlled 360° rotation and a linear servo (M3) for moving the folding arm into and out of the plane of folding. The stop is made from two parallel carbon fibre rods. A heat gun (XL3000, Sparkfun, USA) is mounted on a frame over the region between the stop and the folding arm and is powered by 110-V A/C electricity through a powerswitch tail. In this study, the distance between the centre of the rollers and the stop along the central axis is 13.5 cm, the distance between the centre of the folding arm range circle and the stop along the central axis is 1.5 cm, and the folding arm range circle has a radius of 1 cm.

C. A Hexapedal Robot

The hexapod is based on the open-source robot Open-RoACH. The untethered legged robot measures 15 cm long, 11 cm wide, and 250 grams including a 7.4V Li-Po battery. It has two DC motors (Micro Metal Gearmotors, Pololu, USA) driving six legs. It has an onboard microcontroller (mbed LXP LPC1768, ARM, UK), a linescan sensor (TSL1401, Parallax, USA), and an inertial measurement unit (IMU) (GY-521 MPU-6050, Phantom YoYo, China). All the original six legs are made from the same sandwich structure as the ribbon, manually folded into a square shape. Each of the legs is attached to the main body of the robot with a pair of permanent magnets. There are two more magnets mounted on a supporting structure over the robot, serving as the engagement mechanism with the regenerating robot.

III. Modelling of Folded Joint Stiffness

Automatic regeneration based on the ribbon-folding scheme can generate structures with the same shape and dimension as the original, or structures with a different dimension or shape. To understand the mechanical properties of the various structures that could be regenerated, individual folded joints need to be modelled. As one of the three functional components on the ribbon, the shape-changing joints can be folded into joints with certain resting angles. The stiffness of these folded joints determines the rigidity of the regenerated structures.

Fig. 4 shows the joint with two adjacent links on the left. It is assumed the middle PET layer of the joint is so thin that its effect on stiffness is negligible, hence the joint is treated as a

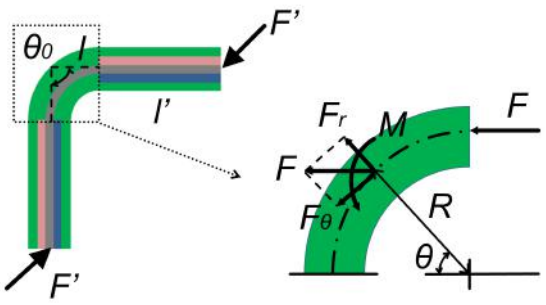

Fig. 4. A curved beam model for a folded shape-changing joint.

homogeneous curved beam, as shown on the right. By using Castigliano's theorem, we can find the deflection δ of the joint (not shown in Fig. 4) due to a load F, in the direction of F and at its point of application [30]. Consider the strain energy in the element defined by the angle $d\theta$ located at an angle θ with respect to the direction of F, the total strain energy is:

$$U = \int dU_1 + \int dU_2 + \int dU_3 + \int dU_4 \qquad (1)$$

The required deflection is:

$$\delta = \frac{\partial U}{\partial F} = \int_0^{\theta_0} \frac{M}{AeE}\left(\frac{\partial M}{\partial F}\right) d\theta + \int_0^{\theta_0} \frac{F_\theta R}{AE}\left(\frac{\partial F_\theta}{\partial F}\right) d\theta - \int_0^{\theta_0} \frac{1}{AE}\left(\frac{\partial M F_\theta}{\partial F}\right) d\theta + \int_0^{\theta_0} \frac{CF_r R}{AG}\left(\frac{\partial F_r}{\partial F}\right) d\theta$$

For the specific case in Fig. 4, substituting $F_r = F\cos\theta$, $F_\theta = F\sin\theta$, $M = FR\sin\theta$ and $MF_\theta = F^2 R\sin^2\theta$ into the above equation yields:

$$\delta = \frac{FR^2}{AeE}\int_0^{\theta_0} \sin^2\theta d\theta - \frac{FR}{AE}\int_0^{\theta_0} \sin^2\theta d\theta + \frac{CFR}{AG}\int_0^{\theta_0} \cos^2\theta d\theta \qquad (2)$$

where θ_0 is the resting angle of the folded joint, A is the cross-sectional area of the beam, R is the radius of the centroidal axis of the curved beam, E and G are the elastic and the shear modulus of the material, $e = R - r_n$ is the eccentricity between the centroidal axis and the neutral axis, and C is the cross-section correction factor and equals 1.5 for a rectangular cross-section.

IV. Experiments and Results

A. Joint Stiffness Model Validation

1) Method: To validate the stiffness model, 60 samples of flexure joints with four resting angles (θ_0=30°, 60°, 90°, 120°) and three widths (4 mm, 8 mm, 16.6 mm) were made by laser cutting, laminating and manual folding. The HMA (Surebonder 711R510, Wauconda, IL, USA) used in making the samples has an elastic (E) and a shear modulus (G) of approximately 80 MPa.

The joints had adjacent links with a length of l'=20 mm. In terms of thickness, the 30° samples had a thickness of 2.48±0.12 mm, 2.93±0.32 mm and 3.90±0.31 mm for the three widths (4, 8, 16.6 mm respectively); the 60° samples had a thickness of 1.49±0.09 mm, 2.20±0.17 mm and 2.60±0.33 mm for the three widths; the 90° samples had a thickness of 1.33±0.05 mm, 1.82±0.18 mm and 2.19±0.12 mm for the three widths; and the 120° samples had a thickness of 1.17±0.06 mm, 1.49±0.05 mm and 1.99±0.13 mm for the three widths. The PET layer had a thickness of 0.076 mm, which is negligible compared to the overall thickness of the joint, hence the joints were treated as homogeneous HMA. It is assumed the PET layer is not stretched during folding and it serves as the neutral axis with a length of 1.15 mm.

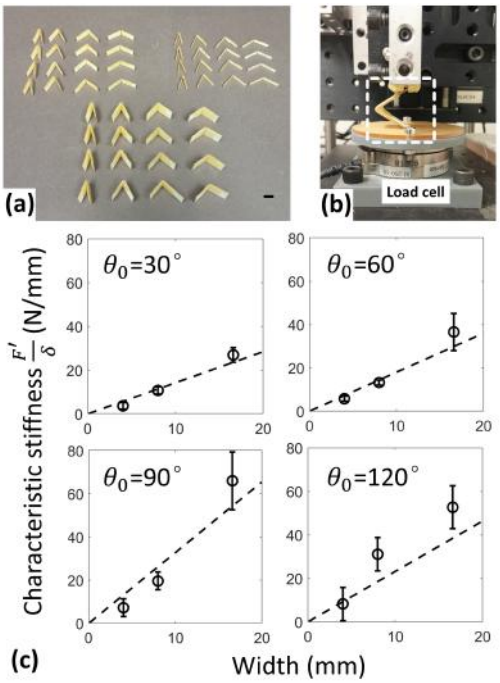

Fig. 5. (a) Example fabricated structures. (b) Joint stiffness measurement apparatus. (c) Results of characteristic joint stiffness in terms of the flexure width and the resting angle. Dashed lines are model predictions based on Equation 2.

All the samples were tested on a step-motor actuated three-axis apparatus built from Newport optical components. A six-axis load cell (ATI SI-290-10, Apex, NC, USA) was used to collect force data at a frequency of 1500 Hz. The samples were fixed between the apparatus and the load cell. Compression tests were carried out with a rate of 0.5 mm/s. Fig. 5 a&b shows the samples and one of them being fixed on the testing apparatus.

The compression stiffness was characterized as the ratio between measured vertical force at the end of the links (F' in Fig. 4) and estimated deflection of the joint (δ). The deflection of the joint was estimated as follows:

$$\delta = \frac{l\delta'}{l + l'} \qquad (3)$$

where δ' is measured vertical displacement and

$$l = \frac{R}{\tan(\theta_0/2)} \tag{4}$$

$$R = \frac{s}{\pi - \theta_0} + e \tag{5}$$

where s is the length of the neutral axis.

2) Result: Fig. 5 shows characteristic stiffness of joint compression for the four resting angles across width. The following values were selected for eccentricity e: 5×10^{-8} mm for 30°, 1×10^{-6} mm for 60°, 1×10^{-5} mm for 90°, and 3×10^{-5} mm for 120°. It can be seen that the model predicts the stiffness reasonably well. Stiffness increases with the width and the resting angle and its peak occurs at 90° across different resting angles. For a joint width of 10 mm, the characteristic stiffness was between 15 and 30 N/mm. Deviation could be caused by a number of factors including the bending of the adjacent links, the direction of compression forces, and the error in eccentricity fitting.

B. Demonstration of Automatic Leg Regeneration

1) Method: To demonstrate automatic leg regeneration, the regenerating robot and the legged robot cooperate based on feedbacks from the proximity sensor and the IMU. The former provides triggering signals to activate or deactivate the regenerating robot, while the latter provides triggering signals for the legged robot to move on the ground or stop moving when it is being repaired.

For leg regeneration, an open-loop sequence controlled the regenerating robot for positioning, orienting, detachment, fabrication and attachment (Fig. 6a). First the sequence enters a positioning and orienting process, where it lifts up the legged robot with M7, orients it in the horizontal plane with M8 and positions it in the horizontal plane with M4-M6. When there is a damaged leg, the sequence enters a leg detachment process, where M4-M7 work together with the detachment arm to pull the leg off. Then the sequence enters the fabrication process, where the regenerating robot switches between two positions for M3, gives angular position commands to M2 based on the folding angle, and angular displacement commands to M1 based on the length of each link of the structure. It also turns on the powerswitch tail for heating or waits a certain duration for passive cooling. The controller subsequently enters an attachment process, in which it lowers M3, gives an angular displacement command to M1 and turns on the powerswitch tail for heating. Lastly the sequence returns the legged robot to its initial position and orientation in the horizontal plane, lifts it further up to disengage the legged robot and returns to its initial height.

The regenerated leg was chosen to have the same shape as the original i.e. a planar square and with the same dimension. The dimension of square used in this study is: three edges of the square measured 3 cm long and the fourth edge was 7 cm long. The ribbon was 8.4 mm wide and it contained segments matching the length of the edges of the square. For the controller, heating and cooling were predefined as 13 seconds and 60 seconds respectively. Other control parameters were predefined according to the edge lengths and folding angles at each step.

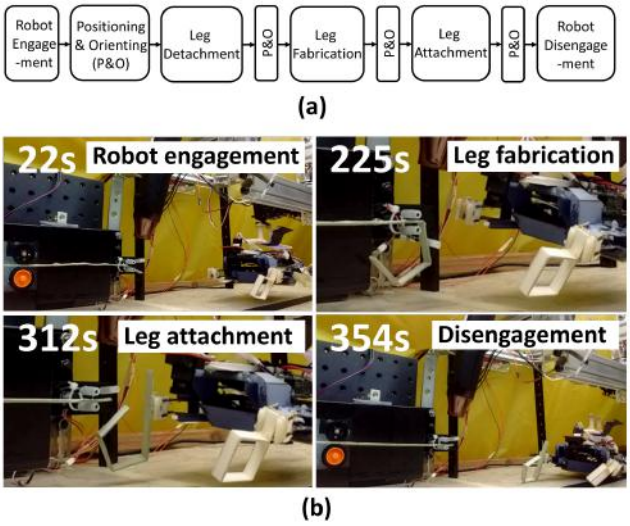

Fig. 6. (a) Regeneration sequence. (b) Snapshots of automatic regeneration of a leg in the hexapod. During 0-44 seconds, the legged robot with a missing front right leg approached the regenerating robot, engaged and positioned. During 44-312 seconds, the regenerating robot fabricated a new square leg on-the-fly, delivered the leg to be attached to the legged robot. During 312-354 seconds, the legged robot was repositioned and disengaged from the regenerating robot. During 354-362 seconds, the legged robot walked away.

2) Result: Fig. 6b shows snapshots of an automatic process of cooperative repairing. Initially the legged robot suffered loss of its front right leg. It was still capable of moving but at a lower speed. It used a linescan sensor to follow a path to approach the regenerating robot. At the 19th second the legged robot engaged with the regenerating robot, and the latter entered the regeneration operation with the feedback from its proximity sensor. At the 22nd second, the legged robot got lifted up and stopped movement with the feedback from its IMU. From the 22nd to the 44th second, the regenerating robot positioned the legged robot. At the 76th, the 150th, and the 225th second, the regenerating robot finished the folding of the first, the second, and the third sides of the square leg. At the 280th second, the regenerating robot delivered the fabricated leg to the legged robot. From the 286th to the 312th second, the fabricated leg was disconnected from the rest of the ribbon and attached to the legged robot with permanent magnets. From the 312th to the 334th second, the regenerating robot return the legged robot to its previous position. From the 339th to the 340th second, the regenerating robot lifted the legged robot further up and disengaged the latter. From the 354th to the 362nd second, the legged robot walked away.

C. Repeatability

1) Method: Each of the three processes of positioning and orienting, leg detachment and robot disengagement was run individually and automatically with predefined control parameter values. Success rate was measured from a total number of 40, 40, and 30 trials respectively.

TABLE II

SUCCESS RATE OF PROCESSES

Positioning	Leg Detachment	Leg Fabrication	Disengagement
40/40	36/40	10/10	30/30

For leg fabrication, ten samples of ribbons were prepared for automatic fabrication of a square structure. The ribbons had a width of 8 mm and thickness of 2mm, with a flexure length of 1.15 mm. Three of the sides of the square have a length of 30 mm while the fourth side extends to the rest of the ribbon. Resulting angles for each fold on each sample were measured.

2) Result: As shown in Table II, the process of robot positioning and orienting and the process of robot disengagement achieved a 100% success rate. The process of leg detachment succeeded 36 trials out of 40. In the four failed trials, the separation between the magnets was not complete and the leg was attracted back to the rest of the legged robot.

For fabrication, when all the ten samples are considered, the first fold gave an angle of 88.9°±13.1°; the second fold gave an angle of 93.8°±12.9°; and the third fold gave an angle of 103.2°±7.5°. For each individual samples, the mean and the standard deviation of the three folded angles were 90.7°±8.3°, 102.7°±10.8°, 98.3°±17.5°, 112.0°±9.8°, 92.7°±10.3°, 93.0°±19.0°, 88.3°±15.4°, 87.7°±4.9°, 97.7°±3.2°, 90.0°±14.4°. The mean of the standard deviation of the ten samples were 11.4°.

D. Effect of Leg Regeneration on Mobility Recovery

1) Method: Effect of leg regeneration on mobility reovery was assessed with the legged robot walking on a flat horizontal tile surface under three conditions: with the intact original legs, without the front right leg, with a regenerated front right leg (Fig. 7). The robot used its linescan sensor to try to follow a straight line in all cases. Kinematics data of the robot were collected using a motion capture system (Optitrack, USA). Power consumption data were collected by tethering the robot to a 9.3-V external power supply and a current sensor (ACS712) sampling at a frequency of 10 Hz. Three trials were run for each leg condition. To quantify mobility, three measures are used, i.e. average forward speed along the line, average peak power, and cost of transport which is the ratio between the energy consumption and the product of weight and travelling distance.

2) Result: Fig. 8 shows the mean and standard deviation values for average forward speed, average peak power, and cost of transport under the three leg conditions. The average forward speed with an intact, a lost and a regenerated front right leg was 0.010±0.001 m/s, 0.004±0.002 m/s,and 0.009±0.002 m/s respectively, suggesting a 60.0% reduction in speed due to leg loss and a 90.0% recovery after regeneration. The average peak power with an intact, a lost and a regenerated front right leg was 17.07±0.59 W, 24.67±5.41 W and 20.44±1.39 W respectively, suggesting an increase of 44.5% of peak power due to leg loss and only an increase of 19.7% of peak power after regeneration. The cost of transport

Fig. 7. A legged robot used in the experiment with its front right leg being intact, lost, and regenerated.

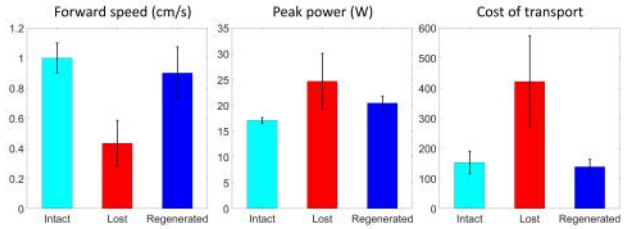

Fig. 8. Results showing mobility recovery in average forward speed, average peak power, and total cost of transport.

with an intact, a lost and a regenerated front right leg was 153.4±37.4, 422.1±151.5 and 139.2±23.9 respectively, suggesting an increase of 175.2% of cost of transport due to leg loss and a surprising reduction of 9.3% after regeneration.

V. CONCLUSIONS AND FUTURE WORK

The paper proposes regeneration in a robotic system for automatic repair, which differs from the state-of-the-art modular approach in that it integrates a fabrication process on the fly. With a system that consists of a regenerating robot, a legged robot and a pre-engineered ribbon, we demonstrate end-to-end execution of automated repair of the legged robot's leg by the regenerating robot in 335 seconds. Experiments on repeatability show a 100% success rate for sub-processes such as positioning, leg fabrication, and legged robot disengagement and a 90% success rate for leg detachment. We quantify the effect of leg regeneration on mobility recovery and found a 90% recovery of forward speed, a 19.7% increase of peak power and a 9.3% reduction of cost of transport with a regenerated leg. The work serves as another evidence that integration of fabrication on-the-fly is beneficial for a robotic system [3], [26].

Future work may be done in a number of directions. From the technical perspective, the scalability of the approach should be demonstrated e.g. by using the present system for automatic regeneration of two or more legs and other structures such as footpads or hips, or by using a larger system; automatic diagnosis and motion planning can be integrated for autonomous structure regeneration; the mechanism design of the regenerating robot may be modified and minimized to be mounted on a mobile platform; and active elements may be embedded in the pre-engineered ribbon for automatic regeneration of sensors or motors. From the scientific perspective, a theory needs to be developed to describe various aspects of regeneration from mechanics, energetics, complexity, granularity to resilience; and the effect of regeneraton on locomotion mechanics and efficiency could be investigated to shed lights on biology research.

REFERENCES

[1] M. Asada, K. Hosoda, Y. Kuniyoshi, H. Ishiguro, T. Inui, Y. Yoshikawa, M. Ogino, and C. Yoshida, "Cognitive developmental robotics: A survey," IEEE Trans. Auton. Ment. Dev., vol. 1, no. 1, pp. 12-34, May 2009.

[2] Y. Jin and Y. Meng, "Morphogenetic robotics: An emerging new field in developmental robotics," IEEE Trans. Syst. Man Cybern. Part C-Appl. Rev., vol. 41, no. 2, pp. 145-160, Mar. 2011.

[3] L. Wang, "Shape adaptation through soft-matter extended phenotype enhances robots' functionality," Dr.sc. dissertation, Dept. Mech. Process Eng., ETH Zurich, Switzerland, 2014.

[4] M. Yim, W.-M. Shen, B, Salemi, D. Rus, M. Moll, H. Lipson, E. Klavins, and G. S. Chirikjian, "Modular self-reconfigurable robot systems," IEEE Robot. Autom. Mag., vol. 14, no. 1, pp. 43-52, Mar. 2007.

[5] R. Gross and M. Dorigo, "Self-assembly at the macroscopic scale," Proc. IEEE, vol. 96, no. 9, pp. 1490-1508, Sep. 2008.

[6] M. Rubenstein, Y. Sai, C.-M. Chuong, and W.-M. Shen, "Regenerative patterning in Swarm Robots: mutual benefits of research in robotics and stem cell biology," Int. J. Dev. Biol., vol. 53, no. 5-6, pp. 869-881, 2009.

[7] R. Thenius, M. Dauschan, T. Schmickl, and K. Crailsheim, "Regenerative abilities in modular robots using virtual embryogenesis," in Proc. 2nd Int. Conf. Adaptive and Intelligent Systems, Klagenfurt, Austria, pp. 227-237, 2011.

[8] K. E. McLean and M. K. Vickaryous, "A novel amniote model of epimorphic regeneration: the leopard gecko, Eublepharis macularius," BMC Dev. Biol., vol. 11, no. 50, 2011.

[9] A. Avizienis, G. Gilley, F. Mathur, D. Rennels, J. Rohr, and D. Rubin, "The STAR (Self-Testing And Repairing) computer: An investigation of the theory and practice of fault-tolerant computer design," IEEE Trans. Comput., vol. C-20, no. 11, pp. 1312-1321, 1971.

[10] R. Frei, R. McWilliam, B. Derrick, A. Purvis, A. Tiwari, and G. D. M. Serugendo, "Self-healing and self-repairing technologies," Int. J. Adv. Manuf. Technol., vol. 69, no. 5, pp. 1033-1061, Nov. 2013.

[11] M. Yim, B. Shirmohammadi, J. Sastra, M. Park, M. Dugan, and C. J. Taylor, "Towards robotic self-reassembly after explosion," in Proc. 2007 IEEE/RSJ Int. Conf. Intelligent Robots Systems, San Diego, USA, pp. 2767-2772.

[12] M. D. M. Kutzer, M. Armand, D. H. Scheidt, E. Lin, and G. S. Chirikjian, "Toward cooperative team-diagnosis in multi-robot systems," Int. J. Robot. Res., vol. 27, no. 9, pp. 1069-1090, Sep. 2008.

[13] T. Fukuda and S. Nakagawa, "Dynamically reconfigurable robotic system," in Proc. 1988 IEEE Int. Conf. Robotics Automation, Philadelphia, USA, pp. 1581-1586.

[14] E. Yoshida, S. Murata, K. Tomita, H. Kurokawa, and S. Kokaji, "Distributed formation control for a modular mechanical system," in Proc. 1997 IEEE/RSJ Int. Conf. Intelligent Robots Systems, Grenoble, USA, pp. 1090-1097.

[15] R. Fitch, D. Rus, and M. Vona , "A basis for self-repair robots using self-reconfiguring crystal modules," in Proc. 6th Int. Conf. Intelligent Autonomous Systems, Venice, Italy, 2000, pp. 903-910.

[16] K. Stoy and R. Nagpal, "Self-repair through scale independent self-reconfiguration," in Proc. 2004 IEEE/RSJ Int. Conf. Intelligent Robots Systems, Sendal, Japan, pp. 2062-2067.

[17] D. J. Christensen, "Evolution of shape-changing and self-repairing control for the ATRON self-reconfigurable robot," in Proc. 2006 IEEE Int. Conf. Robotics Automation, Orlando, USA, pp. 2539-2545.

[18] W.-M. Shen, P. Will, and A. Galstyan, "Hormone-inspired self-organization and distributed control of robotic swarms," Auton. Robot., vol. 17, no. 1, pp. 93-105, Jul. 2004.

[19] J. Cheng, W. Cheng and R. Nagpal, "Robust and self-repairing formation control for swarms of mobile agents," in Proc. 20th Nat. Conf. Artificial intelligence, Pittsburg, USA, 2005, pp. 59-64.

[20] D. J. Arbuckle and A. A. G. Requicha, "Self-assembly and self-repair of arbitrary shapes by a swarm of reactive robots: algorithms and simulations," Auton. Robot., vol. 28, no. 2, pp. 197-211, Feb. 2010.

[21] E. Yoshida, S. Murata, K. Tomita, H. Kurokawa, and S. Kokaji, "An experimental study on a self-repairing modular machine," Robot. Auton. Syst., vol. 29, no. 1, pp. 79-89, Oct. 1999.

[22] C. Bererton and P. K. Khosla, "Towards a team of robots with reconfiguration and repair capabilities," in Proc. 2001 IEEE Int. Conf. Robotics Automation, Seoul, South Korea, pp. 2923-2928.

[23] J. D. Davis, Y. Sevimli, M. K. Ackerman, and G. S. Chirikjian, "A robot capable of autonomous robotic team repair: The Hex-DMR II system," in Proc. 3rd IEEE/IFToMM Int. Conf. Reconfigurable Mechanisms and Robots, Beijing, China, 2015, pp. 619-631.

[24] R. MacCurdy, R. Katzschmann, Y. Kim, and D. Rus, "Printable hydraulics: A method for fabricating robots by 3D co-printing solids and liquids," in Proc. 2016 IEEE Int. Conf. Robotics Automation, Stockholm, Sweden, pp. 3878-3885.

[25] L. Brodbeck, L. Wang, and F. Iida, "Robotic body extension based on hot-melt adhesives," in Proc. 2012 IEEE Int. Conf. Robotics Automation, St Paul, USA, pp. 4322-4327.

[26] L. Wang, L. Brodbeck, and F. Iida, "Mechanics and energetics in tool manufacture and use: a synthetic approach," J. R. Soc. Interface, vol. 11, no. 100, pp. 20140827, Nov. 2014.

[27] L. Wang, M. Plecnik, and R. S. Fearing, "Robotic folding of 2D and 3D structures from a linear ribbon," in Proc. 2016 IEEE Int. Conf. Robotics Automation, Stockholm, Sweden, pp. 3655-3660.

[28] A. Nagabandi, L. Wang, and R. S. Fearing, "A path planning algorithm for single-ended continuous planar robotic ribbon folding," in Proc. 2016 IEEE/RSJ Int. Conf. Intelligent Robots Systems, Daejeon, South Korea, 3239-3246.

[29] A. M. Hoover and R. S. Fearing, "Fast scale prototyping for folded millirobots," in Proc. 2008 IEEE Int. Conf. Robotics Automation, Pasadena, USA, pp. 886-892.

[30] R. G. Budynas and J. K. Nisbett, Shigleys Mechanical Engineering Design (Ninth Edition). New York, NY: McGraw-Hill, 2011, pp. 169-171.